Journal of Tissue Engineering
Volume 11: 1–13

DOI: 10.1177/2041731420963981
journals.sagepub.com/home/tej
SAGE

3D brain tissue physiological model with co-cultured primary neurons and glial cells in hydrogels

Ilaria Raimondi[1], Marta Tunesi[1], Gianluigi Forloni[2], Diego Albani[2] and Carmen Giordano[1]

Abstract

Recently, researchers have focused on the role of gut microbiota on human health and reported the existence of a bidirectional relationship between intestinal microbiota and the brain, referred to as microbiota-gut-brain axis (MGBA). In this context, the development of an organ-on-a-chip platform recapitulating the main players of the MGBA would help in the investigations of the biochemical mechanisms involved. In this work, we focused on the development of a new, hydrogel-based, 3D brain-like tissue model to be hosted in the brain compartment of the aforementioned platform. We previously cultured primary mouse microglial cells, cortical neurons and astrocytes independently, once embedded or covered by a millimeter layer of two selected collagen-based hydrogels. We evaluated cell metabolic activity up to 21 days, cell morphology, spatial distribution and synapse formation. Then, we exploited the best performing culturing condition and developed a more complex brain-like tissue model based on the co-culture of cortical neurons and glial cells in physiological conditions. The obtained results indicate that our 3D hydrogel-based brain tissue model is suitable to recapitulate in vitro the key biochemical parameters of brain tissue.

Keywords

Brain in vitro models, neural cells, 3D culture, hydrogels, collagen

Date received: 7 June 2020; accepted: 13 September 2020

Introduction

Mammalian brain tissue is complex, and challenging to model in vitro. However, the investigations of several pathophysiologic mechanisms would greatly benefit from the availability of reliable cell-based systems featuring at least the main brain cell populations, neurons and glial cells. An example where such models could help move our knowledge forward is the microbiota-gut-brain axis (MGBA). In the last few years, the number of publications on the role of gut microbiota in human health has increased significantly and researchers have reported a bidirectional relationship between gut microbiota and the brain. It exploits several communication pathways, such as the release of microbial factors, intestinal hormones and cytokines from the immune system.[1–4] In this context, the Authors aim at developing an optically accessible multi-organ-on-a-chip platform hosting advanced two- (2D), suspended, and three-dimensional (3D) in vitro models to recapitulate the main players of the MGBA, such as the microbiota, the gut, the immune system, the blood-brain barrier and the brain, in physiological and pathological conditions.[4] In the present work, we focused on the setting up of a millimeter-thick brain-like tissue model potentially suitable for dynamic culture in a recently developed optically accessible organ-on-a-chip (OOC) device.[5]

In the last decade, OOC technology has seen considerable improvements for its potential to reduce animal studies for drug development and toxicity testing.[6] Its reliability and reproducibility offer substantial advantages for tissue

[1]Department of Chemistry, Materials and Chemical Engineering "G. Natta", Politecnico di Milano, Milan, Italy
[2]Department of Neuroscience, Istituto di Ricerche Farmacologiche Mario Negri IRCCS, Milan, Italy

Corresponding author:
Carmen Giordano, Department of Chemistry, Materials and Chemical Engineering "G. Natta", Politecnico di Milano, P.za Leonardo da Vinci 32, 20133 Milan, Italy.
Email: carmen.giordano@polimi.it

and disease modeling,[7,8] overcoming the limitations of 2D static cultures.

Despite their simplicity compared to the *in vivo* situation, 3D models have significantly contributed to the recapitulation of tissue properties, cell-cell contacts and cell-extracellular matrix (ECM) interactions.[9–12] Organoids, miniaturized self-organized tissue cultures from stem cells, are among the most promising 3D models for brain representation.[13,14] They have been employed to study brain development and organization, as well as neurological diseases.[15] However, they lack cell aging[16] and internal vascularization, inducing necrosis.[17] They are hard to grow, labor-intensive and time-consuming, all major disadvantages for investigations of disease pathways and drug targets.[18]

As an alternative to organoids, hydrogels are excellent candidates to mimic the ECM of soft tissues and have emerged for the development of 3D brain-like tissue models.[19] Their stiffness is a key factor in the regulation of neuronal cell shape, viability, expression, migration and differentiation, both in 2D[20,21] and 3D conditions.[22] Several studies have indicated that softer gels promote neurite outgrowth,[23] while glial cells prefer a stiffer microenvironment.[24] However, some studies reported that soft hydrogels support astrocyte differentiation and survival.[25]

Microglia, the resident immune cells of the central nervous system (CNS), play a key role in the maintenance of CNS homeostasis and in the management of tissue response to injury.[26] They are involved in monitoring synapse extension[27] and remodeling during development,[28] they contribute to neuroprotection and regeneration by releasing cytokines, molecules and other neurotrophic factors.[29] Studies coupling microglia and hydrogels are not numerous. Up to now, they have focused on hydrogel effects on cell morphology, adhesion and motility,[26] and cytokine release.[30]

Hydrogels have been used to culture neural cells in different 3D conditions. Ylä-Outinen et al. cultured human embryonic stem cell-derived neural cells up to four weeks under PuraMatrix ™ hydrogels. The cells were cultured on laminin-coated microplates for some days, then covered with a hydrogel layer, or encapsulated into the hydrogels after mixing with the polymer solution.[31] Xu et al. proposed a sandwich-based condition, in which the cells were grown at the interface of two hydrogel layers for 21 days.[32]

For a long time, neurons have been cultured alone in biomaterials or devices and the role of glial cells has gone into the background. Now it has clearly emerged that the advanced modeling of brain-like tissues depends on the co-culture of different neural cell populations and the investigations of their interactions.[15] For instance, astrocytes play key roles in neural functions, such as axon growth and direction, synaptogenesis, formation of the blood-brain barrier, and inflammatory responses.[33] Their morphology, proliferation rate and marker expression are governed by 2D or 3D culture conditions, with 3D cultures providing conditions more similar to the *in vivo* situation and allowing early postnatal cells to transit to the differentiated stellate morphology.[33]

Starting from the literature and our previous works with immortalized neuronal cells,[34,35] we employed semi-interpenetrating polymer networks (semi-IPNs) prepared by promoting collagen (COLL) fibrillogenesis in the presence of hyaluronic acid (HA) or poly(ethylene glycol) (PEG) to develop a millimeter-thick brain-like tissue model based on the co-culture of neurons and glial cells. To set up a physiological model, we started from single cultures of primary mouse microglial cells, cortical neurons and astrocytes and compared two culture conditions: (a) a layered-based condition, where a layer of hydrogel covers the cells attached to the microplate; and (b) an embedded-based condition, where the cells are evenly distributed in the polymer solutions during hydrogel preparation. For both conditions, we recorded cell growth and survival up to 21 days, cell morphology and distribution, and synapse formation in neuronal networks. After selecting the most suitable condition, we proposed a more advanced model, co-culturing neurons and glial cells in the embedded-based condition.

Materials

For hydrogel preparation, we purchased reagents from Sigma-Aldrich (St. Louis, MO, USA). We obtained reagents for cell culture from Thermo Fisher Scientific (Waltham, MA, USA) and plasticware from Corning® (Corning, NY, USA).

Experimental procedures

Hydrogel preparation

For the development of 3D models, we cultured brain cells (as single cultures or co-cultures) in semi-IPNs based on COLL and HA (M_w=1 · 10^5 Da, Altergon Italia, Morra De Sanctis, Italy) or COLL and PEG. We used PEG with two molecular weights (M_w): 1.945 kDa (referred to as PEG_{2000}) and 3.270 kDa (referred to as PEG_{3350}).

For all the formulations, we diluted 8 parts (v/v) type I COLL solution (3 mg/mL) from bovine skin with 1 part (v/v) NaOH 0.1 N and 1 part (v/v) 10x phosphate-buffered saline solution (PBS). For COLL-HA gels, we mixed 1 part (v/v) COLL solution with 1 part (v/v) HA solution (5 mg/mL in water, autoclaved at 121 °C for 15 min or with an equivalent time F_0 equal to 13). For COLL-PEG gels, we mixed 3 parts (v/v) COLL solution with 1 part (v/v) PEG solution (2.4 mg/mL in saline, autoclaved). To promote COLL fibrillogenesis, we incubated the polymer solutions at 37 °C for about 1.5 h.

To select the most suitable conditions to establish a brain-like tissue model based on the co-culture of neurons and glial cells, we plated the cells and covered with a 1.5 mm-thick hydrogel layer (layered condition) or we mixed 1 part (v/v) cell suspension with 9 parts (v/v) polymer solutions, and plated 1.5 mm-thick samples (embedded condition).

Primary brain cell cultures

Primary cells were harvested from CD-1 mice (Charles River Laboratories, Calco, Italy). We harvested microglia from 2 to 3 days postnatal mice, and cortical neurons and astrocytes from 2-4 days postnatal mice. We cultured the cells at 37 °C, 5% CO_2.

3D microglial cells

We prepared microglial cultures according to previous studies.[36,37] We removed the meninges and dissected a slice of cortex, minced it, digested it with 0.25% trypsin supplemented with 0.01% DNase I and pipetted it dropwise onto a 70-µm filter. We suspended the cells in Dulbecco's modified eagle medium/Nutrient mixture F-12 Ham (DMEM/F-12), supplemented with 10% fetal bovine serum (FBS), 100 U/mL gentamicin, 100 U/mL penicillin and 100 µg/mL streptomycin, and plated them in flasks. When the cells were confluent (after about 15 days), we incubated them with 0.25% trypsin for 1.5 h, shaking the flasks every 30 min. We washed the adherent microglial cells twice with medium, detached them with 0.25% trypsin-0.02% EDTA, centrifuged them and suspended them in medium.

For layered conditions, we plated 63,000 cells/cm^2 and covered them with a 1.5 mm-thick hydrogel layer. As controls, we plated 63,000 cells/cm^2 on poly-L-lysine coated microplates. For embedded conditions, we mixed 158,000 cells/cm^2 with the polymer solutions and plated 1.5 mm-thick samples.

For both conditions, after COLL fibrillogenesis we added culture medium and changed it every 2 days.

3D cortical neurons

We harvested primary cortical neurons according to Restelli et al.[38] Briefly, we removed the meninges, dissected small slices of cortex and incubated them at 34 °C for 30 min in dissociation medium supplemented with 20 U/mL papain. We added 0.5 mg/mL trypsin inhibitor and dissociated the tissue with a Pasteur pipette. We suspended the cells in Neurobasal medium supplemented with 2% B27, 2 mM L-glutamine, 100 U/mL penicillin and 100 µg/mL streptomycin.

For layered conditions, we plated 242,000 neurons/cm^2, incubated them for 2h at 37 °C, and covered them with a 1.5 mm-thick hydrogel layer. As controls, we plated 242,000 cells/cm^2 on poly-D-lysine coated microplates. For embedded conditions, we mixed 315,000 cells/cm^2 with the polymer solutions and plated samples of 1.5 mm-thick. For both conditions, after COLL fibrillogenesis we added culture medium and refreshed it (50% v/v) every 2-3 days.

3D astrocytes

We dissected a part of the cerebral cortex, removed the meninges and collected the tissue in Hanks' balanced salt solution (HBSS) without calcium chloride and magnesium, supplemented with 2 mM Hepes, 100 U/mL penicillin and 100 µg/mL streptomycin. We incubated it in 0.25% trypsin-0.02% EDTA for 20 min, added complete medium (Minimum Essential medium supplemented with 10% FBS, 6 g/L D-glucose, 100 U/mL penicillin and 100 µg/mL streptomycin) and dissociated it mechanically with a Pasteur pipette. We pipetted it dropwise onto a 40-µm nylon filter, centrifuged it, suspended it in complete medium and plated it in poly-L-lysine coated flasks.

When the mixed primary glial culture was confluent (after about 20 days), we shook the flasks overnight (220 rpm) and changed the medium. To obtain a purified astrocyte culture, the same or the next day we added L-leucine methyl ester (60 mM) to each flask for 90 min to inhibit microglial growth. Then, we washed the flasks with PBS and added fresh medium. The next day, we prepared the samples.

For layered conditions, we plated 52,500 cells/cm^2 and covered them with a 1.5 mm-thick hydrogel layer. As controls, we plated 52,500 cells/cm^2 on poly-L-lysine coated microplates. For embedded conditions, we mixed 105,000 cells/cm^2 with the polymer solutions and plated 1.5 mm-thick samples. For both conditions, after COLL fibrillogenesis we added culture medium and changed it every 2-3 days.

3D cortical neurons and glial cells: embedded co-culture

We harvested the cells as described, but at least one day after shaking, astrocytes were cultured in complete medium for cortical neurons, and to preserve the microglial cells, L-leucine methyl ester was not added. We mixed 32,000 glial cells/cm^2 and 315,000 cortical neurons/cm^2 with the polymer solutions and plated 1.5 mm-thick samples. As controls, we co-cultured 13,200 glial cells/cm^2 and 242,000 neurons/cm^2 on poly-D-lysine coated microplates. After COLL fibrillogenesis, we added culture medium for cortical neurons and refreshed it (50% v/v) every 3 days.

Cell metabolic activity

To assess the ability of hydrogel matrices to support brain cell survival, we examined cell metabolic activity by MTS assay (Promega, Madison, WI, USA). This was done on

days 1, 2 and 5 for microglial cells; on days 7, 14 and 18 for cortical neurons in layered conditions; and on days 7, 14 and 21 for the other conditions. We incubated the samples for 3 h with culture medium supplemented with 10% MTS, then measured their absorbance at 490 nm. We used 1.5-mm thick cell-free gels as control. We ran the assay on at least five samples/group for single cultures and ten samples/group for the co-culture.

Immunocytochemistry and confocal imaging

Immunocytochemistry was done to observe brain cell morphology and spatial distribution at the time points when we measured the highest cell metabolic activity for 2D controls (on day 2 for microglial cells, and on day 14 for cortical neurons, astrocytes and the co-culture).

We removed the culture medium, washed the samples with PBS and fixed them with paraformaldehyde solution (PFA, 4% in PBS), for 24 h. We washed them with Tris-buffered saline supplemented with 0.1% Tween 20 (TBS-T), and blocked them (8–9 h, 4°C) in TBS-T with 4% normal goat serum (NGS), 1 mg/mL bovine serum albumin (BSA), Tris 50 mM, 0.1% gelatin and 0.3 M glycine. After washing the samples with TBS-T, we incubated them (20 h, 4 °C) with primary antibodies, then washed and incubated (10 h, 4 °C) with secondary antibodies. We stained cell nuclei with 0.02 mM Hoechst 33342 (Thermo Fisher Scientific) for observation with a confocal microscope (FV10i, Olympus, Tokyo, Japan). We stained microglial cells with anti-CD11b (1:8000, Biotechne, Minneapolis, MN, USA), and anti-CD68, a pan-macrophage marker (1:200, Bio-Rad Laboratories, Hercules, CA, USA), cortical neurons with anti-neuron-specific β-tubulin III (Tuj-1, 1:500, Sigma-Aldrich), and astrocytes with anti-glial fibrillary acidic protein (GFAP, 1:3000, Millipore, Burlington, MA, USA). As secondary antibodies (1:500, Thermo Fisher Scientific) we used anti-mouse IgG Alexa Fluor® 488, anti-mouse IgG Alexa Fluor® 647, and anti-rabbit IgG Alexa Fluor® 594. As controls, we examined cells in 2D conditions. Only for single cultures of microglial cells, on day 2 we investigated whether hydrogel presence elicited microglial activation by comparison with control cells previously incubated for 24 h with lipopolysaccharide (LPS, from *Escherichia coli* O111:B4, 1 ug/ml, Sigma-Aldrich), a pro-inflammatory stimulus.

Western Blotting

To assess neuronal function, on days 7 and 14 we investigated synapse formation in single cultures of cortical neurons and in the co-culture. To examine the presence of astrocytes, we investigated GFAP expression in the co-culture at the same time points.

We removed the culture medium, washed the samples with PBS, added lysis buffer (with 1% protease inhibitor cocktail), incubated them for 1 h at 4 °C and lysed them with a cell scraper. We vortexed them for about 1 min, then centrifuged them at 4 °C for 5 min at maximum speed and collected the supernatants. To evaluate the effect of 3D embedded conditions on the basal levels of protein expression, we also examined controls in 2D conditions. In view of a possible interference from COLL, protein content was evaluated only for controls, by the bicinchoninic acid assay (BCA, Pierce™, Thermo Fisher). We separated protein extracts by SDS-PAGE and transferred them to a nitrocellulose membrane (Bio-Rad Laboratories). We incubated the membranes overnight at 4 °C with anti-postsynaptic density protein 95 (PSD-95, 1:5000, NeuroMab, Davis, CA, USA), anti-synaptophysin (a presynaptic protein, 1:5000, Synaptic System GmbH, Goettingen, Germany), anti-N-Methyl-D-Aspartate Receptor Subunit NR1 (NR-1, 1:1000, Synaptic System GmbH), anti-GFAP (1:10000), anti-Tuj-1 (1:5000) or glyceraldehyde 3-phosphate dehydrogenase (GADPH, 1:2000, Millipore). Then, we incubated the membranes with the secondary antibodies conjugated to the enzyme horseradish peroxidase. We covered the membranes with luminol solution (EMD Millipore), developed the immunoreactive bands with Firereader V10 PLUS 26M Imaging system (Uvitec Ltd, Cambridge, UK) and quantified them with Image Lab software. The analysis was done in triplicate.

Statistics

The results were reported as mean ± standard deviation (SD) and analyzed with GraphPad Prism® software (GraphPad Software Inc, release 8.0). Two-way analysis of variance (ANOVA) was followed by Tukey's multiple comparisons test for comparisons of the groups and time frames. We considered $p < 0.05$ significant.

Results

3D microglial cells

In the absence of supporting cells like astrocytes, single cultures of primary microglial cells are viable for a very short time[39] and usually tested 48 to 72 h after plating. We therefore limited the evaluation of their metabolic activity to 5 days. However, this was sufficient to appreciate the benefits of hydrogels for extending their culture time.

In layered conditions, metabolic activity (upper panel, Figure 1(a)) was constant ($p > 0.05$) from day 1 to 2 for cells covered with COLL-HA gels, and it decreased with PEG-based gels. From day 2 to 5, it increased for all the matrices ($p < 0.0001$ for all comparisons). The significant increase on day 5 was due to the loss of viability of 2D controls (almost total absence of cells) and the general slowing of cell growth observed for the hydrogels. On day 2, confocal images (upper panel, Figure 1(b)) confirmed

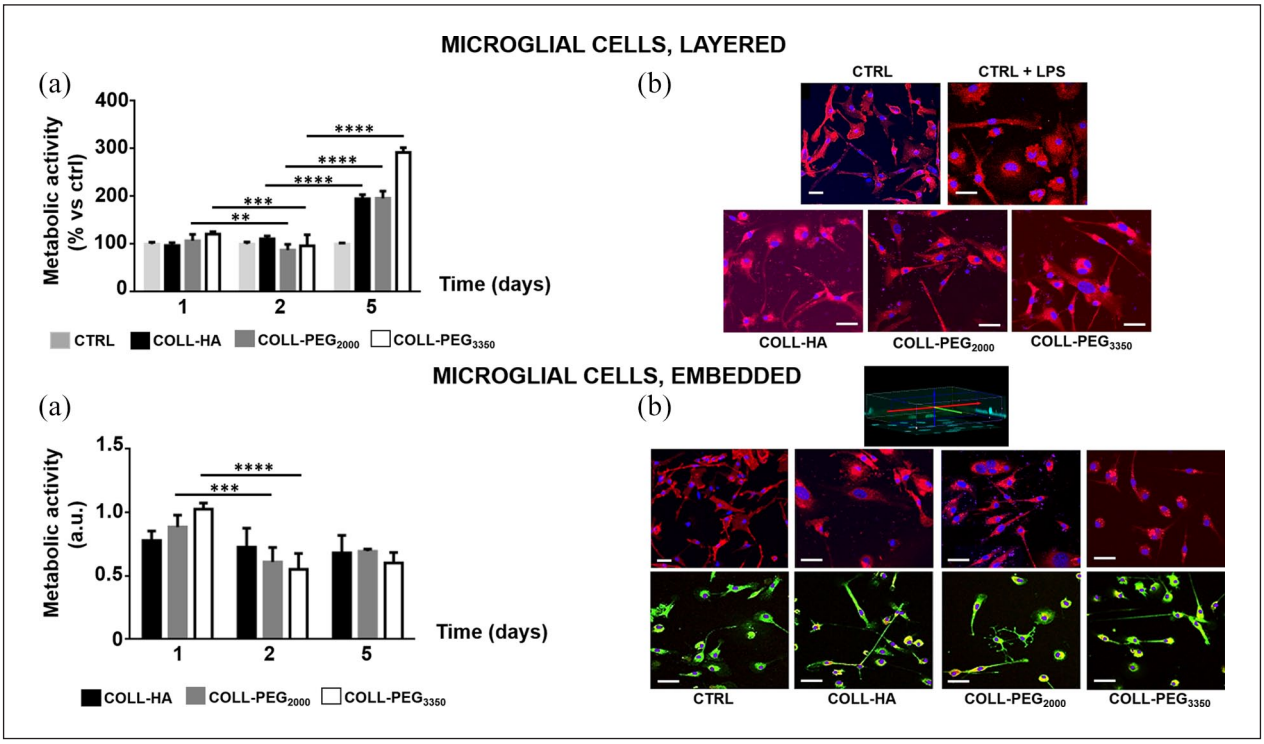

Figure 1. Primary microglial cells in layered and embedded conditions. Layered conditions: (a) Cell metabolic activity over time for microglial cells covered with a 1.5 mm-thick layer of COLL-HA, COLL-PEG$_{2000}$ or COLL-PEG$_{3350}$ gels. The results are mean ± SD with respect to 2D controls (CTRL), 5 replicates/condition. (b) Representative images of microglia immunostained for CD11b (red) and cell nuclei stained with Hoechst 33342 (blue) on day 2. As a reference, cells grown in 2D conditions and incubated with LPS (CTRL + LPS) were also immunostained. Scale bar: 20 μm.
Embedded conditions: (a) Cell metabolic activity over time for microglial cells embedded in 1.5 mm-thick COLL-HA, COLL-PEG$_{2000}$ or COLL-PEG$_{3350}$ gels. The results are mean ± SD, 5 replicates/condition. (b) Representative images of microglia immunostained on day 2. Upper row: cells immunostained for CD11b (red) and cell nuclei stained with Hoechst 33342 (blue); lower row: CD11b (green), CD-68 (red) and cell nuclei stained with Hoechst 33342 (blue). The morphology of CTRL is reported for comparison. Scale bar: 20 μm. For both conditions, cell metabolic activity was analyzed with ordinary two-way ANOVA followed by Tukey's multiple comparisons test.
**$p < 0.01$; ***$p < 0.001$; ****$p < 0.0001$.

uniform cell distribution and nuclei staining indicated that cell number was comparable in all conditions. CD11b staining showed a larger number of branches in the presence of the hydrogels, suggesting the induction of microglial activation. PEG-based matrices showed greater microglial activation than COLL-HA ones, but still lower than positive controls treated with LPS.

In embedded conditions, cell metabolic activity (lower panel, Figure 1(a)) was constant ($p > 0.05$) over time for COLL-HA gels, while for PEG-based semi-IPNs it decreased from day 1 to 2, and then remained constant ($p > 0.05$). CD11b staining (lower panel, Figure 1(b), first set of images) indicated that a few microglia presented a more branched morphology than controls. This suggests that microglial activation is almost absent in embedded conditions. We also assessed microglial phagocytic activity by CD68 staining (red in the second set of images in Figure 1(b)). In COLL-HA and COLL-PEG$_{2000}$ gels, we detected immunoreactivity in the cytoplasm of some microglia, indicating that cell morphology elicited an immune response. For controls and COLL-PEG$_{3350}$ gels, activated cells were almost absent.

3D cortical neurons: Metabolic activity and immunocytochemistry

Experimentally, neuronal cultures are usually employed within 14 days. However, extending this observation time may be important in the view of developing an OOC-based platform for prolonged cell culture and improving the in vitro recapitulation of pathological mechanisms. We therefore extended this target time up to 21 days.

In layered conditions (upper panel, Figure 2(a)), the gels reduced cell metabolic activity compared to 2D controls. Among the matrices, at all the time points PEG-based hydrogels performed best. On day 18, neurons covered with COLL-PEG$_{3350}$ showed the greatest metabolic activity ($p < 0.0001$), while COLL-HA and COLL-PEG$_{2000}$ semi-IPNs gave comparable results ($p < 0.05$). On day 14, for 2D controls and layered cells, Tuj-1 staining (upper

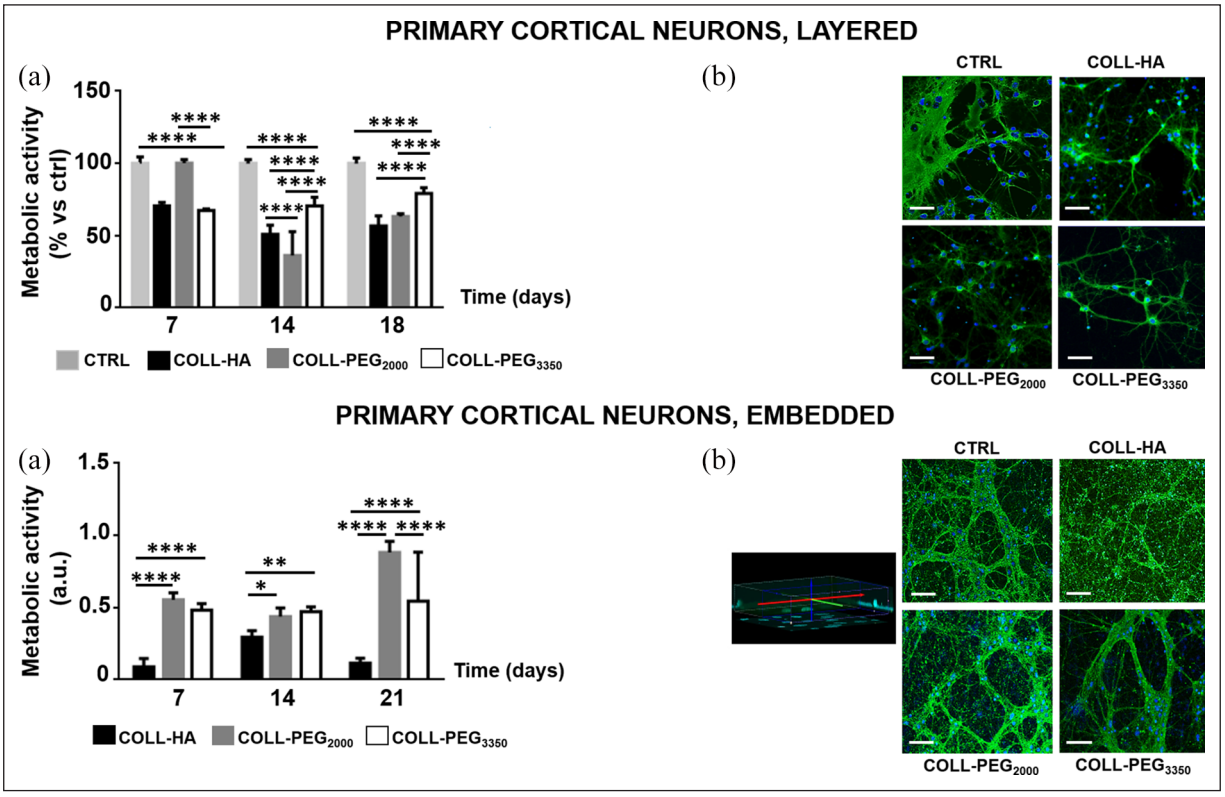

Figure 2. Primary cortical neurons in layered and embedded conditions. Layered conditions: (a) Cell metabolic activity over time for cortical neurons covered with a 1.5 mm-thick layer of COLL-HA, COLL-PEG$_{2000}$ or COLL-PEG$_{3350}$ gels. The results are mean ± SD with respect to 2D controls (CTRL), 8 replicates/condition. (b) Representative images of neurons immunostained for β-tubulin III (Tuj-1, green) and cell nuclei stained with Hoechst 33342 (blue) on day 14. Scale bar: 50 μm.
Embedded conditions: (a) Cell metabolic activity over time for cortical neurons embedded in 1.5 mm-thick COLL-HA, COLL-PEG$_{2000}$ or COLL-PEG$_{3350}$ gels. The results are mean ± SD, 5 replicates/condition. (b) Representative images of neurons immunostained for β-tubulin III (green) and cell nuclei stained with Hoechst 33342 (blue) on day 14. The morphology of CTRL is reported for comparison. Scale bar: 50 μm. For both conditions, cell metabolic activity was analyzed with ordinary two-way ANOVA followed by Tukey's multiple comparisons test.
*$p < 0.05$; **$p < 0.01$; ****$p < 0.0001$.

panel, Figure 2(b)) indicated the presence of articulated neuronal networks and uniform spatial distribution of neuronal extensions, with no aggregated branches. Control neurons had more complex networks. However, neurons covered with PEG-based gels showed more numerous extensions than controls and neurons in COLL-HA semi-IPNs.

Starting from these promising results, we extended the culture time to 21 days for the embedded condition (lower panel, Figure 2(a)). At all the time points, cell metabolic activity was lower for COLL-HA semi-IPNs. Differences between PEG-based gels were found only on day 21, with COLL-PEG$_{2000}$ performing best ($p < 0.0001$). On day 14 (lower panel, Figure 2(b)), 2D controls showed dense neuronal networks. Similar networks were observed in PEG-based semi-IPNs, where neuronal extensions penetrated the matrices and spread in all directions. For COLL-HA gels, MTS assay indicated viable neurons, but Tuj-1 staining showed the almost complete absence of neuronal extensions. DNA staining indicated smaller nuclei than in the other semi-IPNs, suggesting possible cell suffering. These results indicate that the embedded condition promotes the formation of more complex neuronal networks than the layered one. The embedded-based model represents a more physiologically relevant condition and allows cells to benefit from a larger surface area for growth.[40]

3D cortical neurons: Synapse formation

To obtain dense, mature neuronal networks in vitro, generally about 10 days are required.[41] We therefore studied the expression of PSD-95, synaptophysin, and NR-1 on days 7 and 14. Since it is a neuron-specific marker and it is not influenced by cell proliferation, we investigated synapse formation using β-tubulin III as the housekeeping protein. As stress or 3D culture conditions can influence cytoskeleton architecture and thus β-tubulin III expression,[42] before quantification we performed Western blot analysis using GADPH as the housekeeping protein (data not shown).

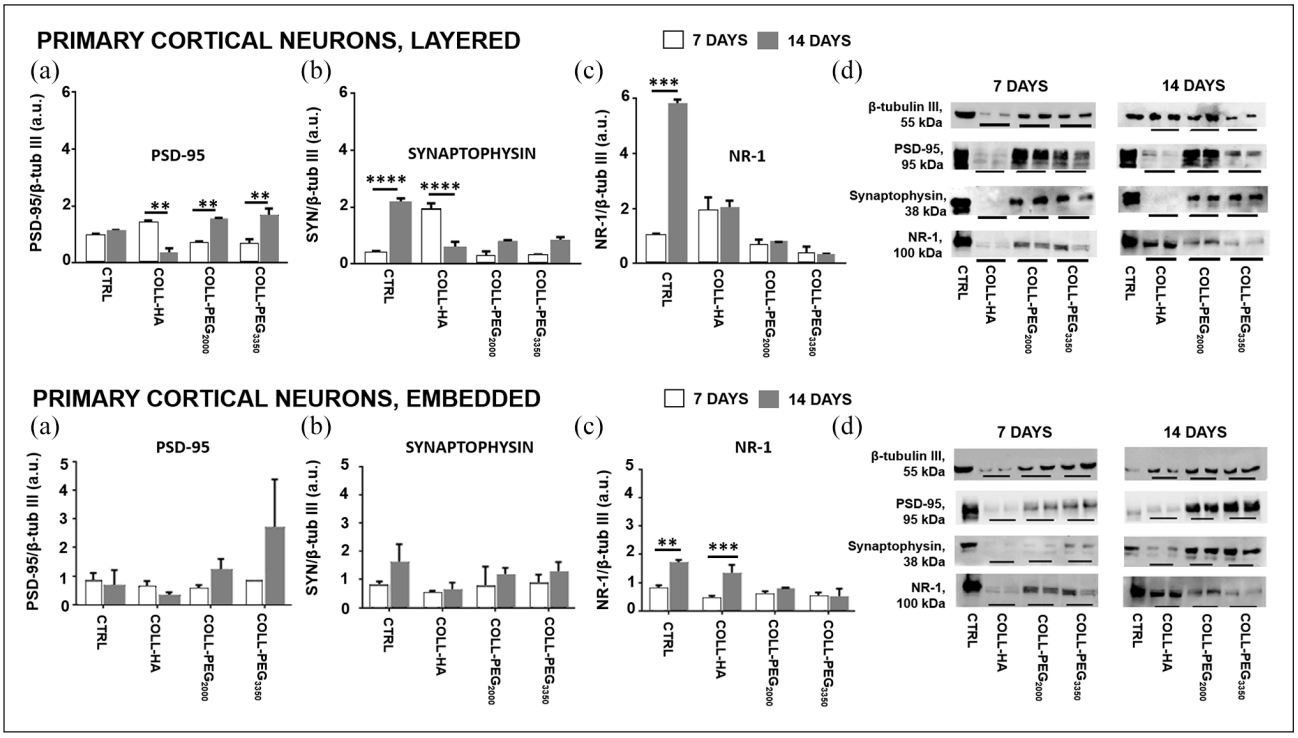

Figure 3. Immunoblots on primary cortical neurons in layered and embedded conditions. Layered conditions: Western blot quantification on days 7 and 14 to detect (a) PSD-95, (b) Synaptophysin, (c) NR-1, in cortical neurons covered with a 1.5 mm-thick layer of COLL-HA, COLL-PEG_{2000} or COLL-PEG_{3350} gels. (d) Representative immunoblots used for the quantifications.
Embedded conditions: Western blot quantification on days 7 and 14 to detect (a) PSD-95, (b) Synaptophysin, (c) NR-1, in cortical neurons embedded in 1.5 mm-thick COLL-HA, COLL-PEG_{2000} or COLL-PEG_{3350} gels. (d) Representative immunoblots used for the quantifications.
The results (mean ± SD, 3 replicates/condition) are also reported for 2D controls (CTRL) and normalized to β-tubulin III (Tuj-1). They were analyzed with ordinary two-way ANOVA followed by Tukey's multiple comparisons test. For CTRL, we loaded 20 µg total proteins, and for each hydrogel, we loaded 20 µL total sample.
*$p < 0.05$; **$p < 0.01$; ***$p < 0.001$.

In layered conditions (upper panel, Figure 3(a)–(d)), the levels of PSD-95 rose from day 7 to 14 for PEG-based gels ($p < 0.01$), but decreased in the presence of COLL-HA ($p < 0.01$). In these matrices, the levels of synaptophysin also decreased ($p < 0.0001$). No differences in the levels of NR-1 were observed for the hydrogels.

In contrast, in embedded conditions (lower panel, Figure 3(a)–(d)), the levels of PSD-95 increased for PEG-based gels from day 7 to 14, but it was not significant ($p > 0.05$). Similarly, for all the matrices the levels of synaptophysin did not change over time ($p > 0.05$). On the contrary, the levels of NR-1 rose for COLL-HA samples ($p < 0.001$).

3D astrocytes

For astrocytes in layered conditions (upper panel, Figure 4(a)), cell metabolic activity was lower than for 2D controls. For all the matrices, cell metabolic activity increased ($p < 0.0001$) between days 7 and 14, but the worst performances were for COLL-HA semi-IPNs. On day 21, metabolic activity was greatest for astrocytes layered with PEG-based gels ($p < 0.0001$). On day 14, confocal images (upper panel, Figure 4(b)) showed uniform cell distribution. For astrocytes covered with COLL-HA gels, nuclear staining indicated a cell number comparable to the other conditions, but GFAP staining suggested that astrocytes had a limited, undeveloped morphology compared to their counterparts covered by PEG-based gels.

In embedded conditions (lower panel, Figure 4(a)), cell metabolic activity was greatest for COLL-HA semi-IPNs ($p < 0.0001$) and no differences were found between PEG-based gels. This suggests slower astrocyte proliferation in PEG-based matrices. Like in layered conditions, on day 14 confocal images (lower panel, Figure 4(b)) showed uniform cell distribution within the gels. In COLL-HA semi-IPNs, nuclei staining indicated a higher cell number than in 2D controls and PEG-based matrices, but GFAP staining suggested that COLL-HA gels disadvantaged astrocytic branching. There were some differences between astrocyte morphology in controls and PEG-based gels, but growth in 3D matrices seemed slower than in 2D conditions.

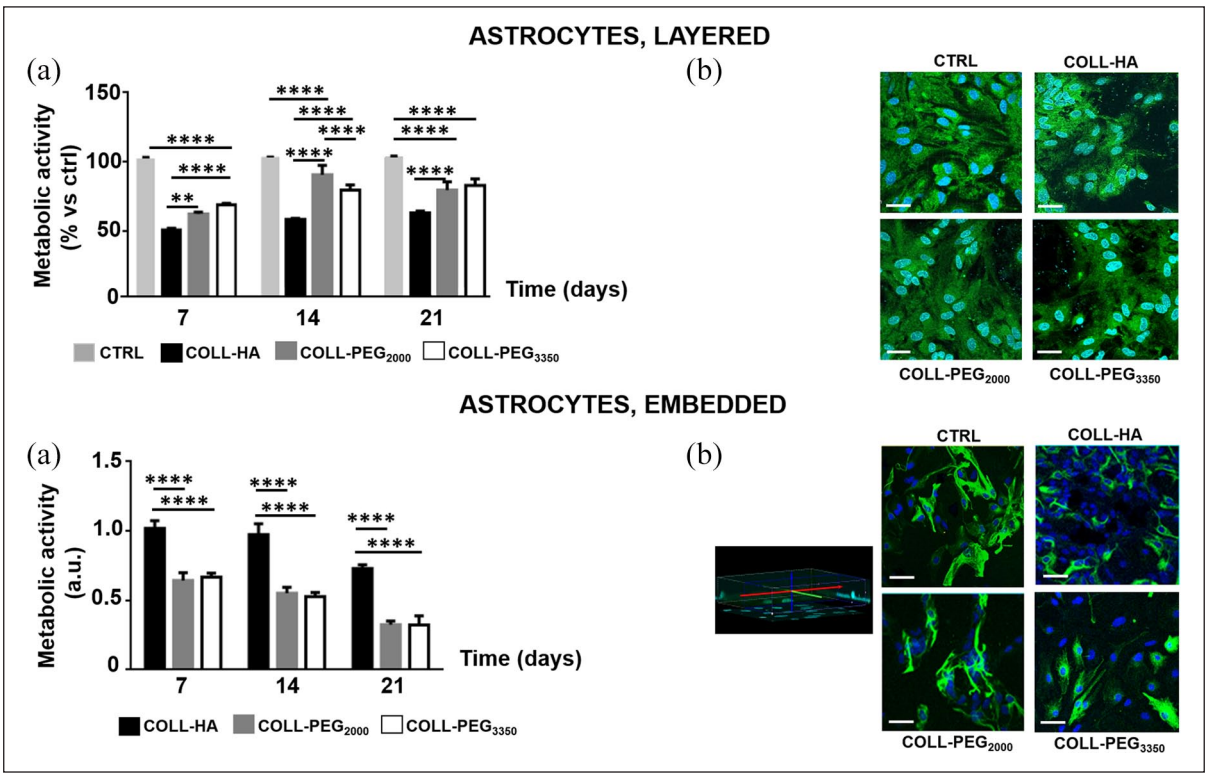

Figure 4. Primary astrocytes in layered and embedded conditions. Layered conditions: (a) Cell metabolic activity over time for astrocytes covered with a 1.5 mm-thick layer of COLL-HA, COLL-PEG$_{2000}$ or COLL-PEG$_{3350}$ gels. The results are mean ± SD with respect to 2D controls (CTRL), 5 replicates/condition. (b) Representative images of astrocytes immunostained for GFAP (green) and cell nuclei stained with Hoechst 33342 (blue) on day 14. Scale bar: 50 μm.
Embedded conditions: (a) Cell metabolic activity over time for astrocytes embedded in 1.5 mm-thick COLL-HA, COLL-PEG$_{2000}$ or COLL-PEG$_{3350}$ gels. The results are mean ± SD, 5 replicates/condition. (b) Representative images of astrocytes immunostained for GFAP (green) and cell nuclei stained with Hoechst 33342 (blue) on day 14. The morphology of CTRL is reported for comparison. Scale bar: 50 μm. For both conditions, metabolic activity was analyzed with ordinary two-way ANOVA followed by Tukey's multiple comparisons test.
$^{**}p < 0.01$; $^{****}p < 0.0001$.

3D neurons and glial cells: Co-culture (metabolic activity and immunocytochemistry)

The previous results indicated that the embedded-based model promotes the formation of more complex neuronal networks and considerably reduces microglial activation. We therefore selected this condition to develop a 3D brain-like tissue model based on the co-culture of cortical neurons and glial cells.

In COLL-HA gels, cell metabolic activity (Figure 5(a)) was constant from day 7 to 14 ($p > 0.05$), then it decreased ($p < 0.01$). In PEG-based matrices, it decreased from day 7 to 14 ($p < 0.0001$), then it rose ($p < 0.05$ for COLL-PEG$_{2000}$; $p < 0.001$ for COLL-PEG$_{3350}$). On day 21, COLL-PEG$_{3350}$ semi-IPNs performed best.

On day 14, confocal imaging showed the presence of complex networks (Figure 5(b)), where glial cells and neurons can communicate. GFAP staining indicated that astrocytes supported neuronal cells, while Tuj-1 staining showed that neural networks are denser than in single cultures. However, spatial organization was more complex in COLL-PEG$_{2000}$ gels. In agreement with nuclear staining, in COLL-HA and COLL-PEG$_{3350}$ matrices, Tuj-1 staining revealed less dense and structured neuronal networks, while GFAP staining showed that glial cells were only partially dedicated to neuronal support.

3D neurons and glial cells: Co-culture (synapse formation)

When co-culturing neurons and glial cells, we measured the levels of synaptic markers in the semi-IPNs at 7 and 14 days (Figure 6(a)–(d)). These suggest that the selected culture conditions permit the maintenance of the key biochemical parameters of the embedded cell populations for a considerable time. In most cases (e.g. PSD-95 in COLL-PEG$_{3350}$, synaptophysin in COLL-PEG$_{2000}$ and NR-1 in COLL-HA gels), we confirmed the previous results for single cultures of cortical neurons in embedded conditions. Furthermore, the changes in expression levels were greater in co-culture conditions than in single cultures. However, for COLL-HA gels protein content was lower than for PEG-based gels (Figure 6(e)). This agrees with previous

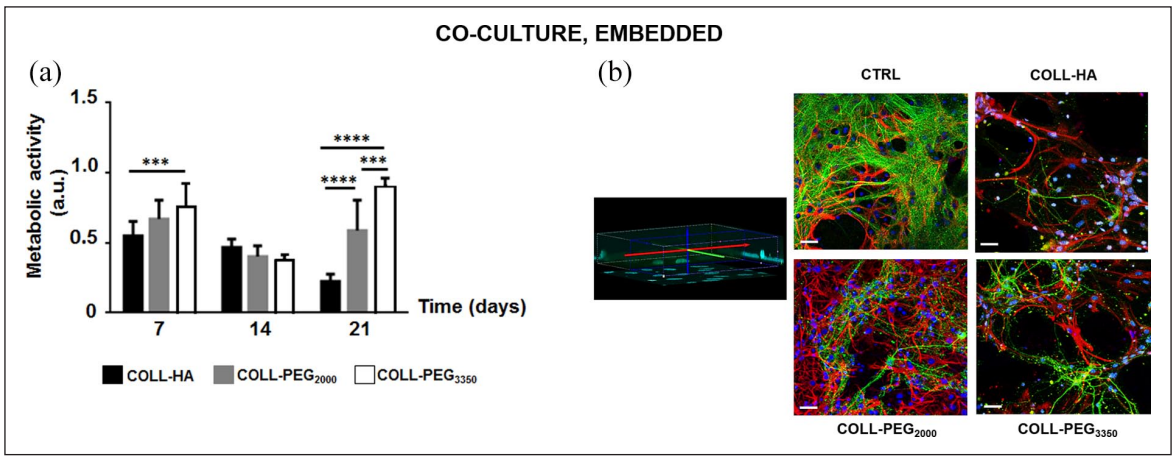

Figure 5. Co-cultures of cortical neurons and glial cells. (a) Cell metabolic activity over time for cortical neurons and glial cells embedded in 1.5 mm-thick COLL-HA, COLL-PEG_{2000} or COLL-PEG_{3350} gels. The results are mean ± SD, 10 replicates/condition. The results were analyzed with ordinary two-way ANOVA followed by Tukey's multiple comparisons test. (b) Representative images of embedded neurons immunostained for β-tubulin III (Tuj-1, green), astrocytes immunostained for GFAP (red) and cell nuclei stained with Hoechst 33342 (blue) on day 14. The morphology of CTRL was reported for comparison. Some nuclei whose cell body was not reactive either to Tuj-1 or GFAP are present, likely belonging to microglial cells. Scale bar: 20 μm.
***$p < 0.001$; ****$p < 0.0001$.

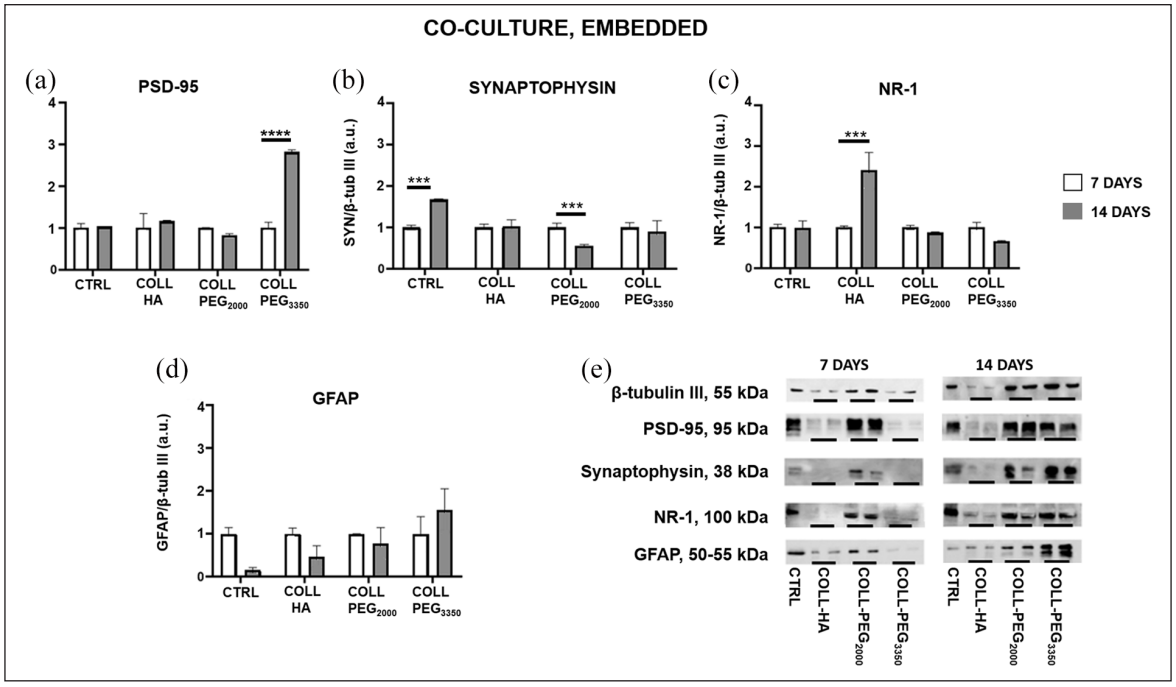

Figure 6. Immunoblots on co-cultures of cortical neurons and glial cells. Western blot quantification on days 7 and 14 to detect (a) PSD-95, (b) Synaptophysin, (c) NR-1, (d) GFAP, in co-cultures of cortical neurons and glial cells embedded in 1.5 mm-thick COLL-HA, COLL-PEG_{2000} or COLL-PEG_{3350} gels. The results (mean ± SD, 3 replicates/condition) are also reported for 2D controls (CTRL) and normalized to β-tubulin III (Tuj-1). They were analyzed with ordinary two-way ANOVA followed by Tukey's multiple comparisons test. (e) Representative immunoblots used for quantification. For CTRL, we loaded 20 μg total protein, and for each hydrogel, we loaded 20 μL total sample.
***$p < 0.001$; ****$p < 0.0001$.

results from cell metabolic activity (Figure 5(a)), but suggests a poor quality of the culture. In COLL-PEG_{3350}, β-tubulin III expression was low on day 7, suggesting slower neuronal maturation than in COLL-PEG_{2000} matrices. However, it rose significantly on day 14. In COLL-PEG_{2000} gels, β-tubulin III increased slightly between days 7 and

14, indicating that these semi-IPNs are more promising to reach the target culture time of 21 days.

To investigate the balance between neurons and glial cells over time, we measured the expression levels of GFAP from days 7 to 14 and noted an increase (although not significant) only for COLL-PEG_{3350} matrices (Figure 6(d)). These results confirm that this matrix promotes astrocyte proliferation, but in the time window examined glial cells do not take over the neuronal network.

Discussion

The bidirectional communication between intestinal microbiota and the brain, referred to as MGBA, has attracted growing interest also for its clinical potential, such as exploiting microbiota-based therapeutics as new strategies to manage neurological diseases and behavioral functions. Several challenges remain before clinical translation,[43] but a reliable OOC platform recapitulating in vitro the main players of the MGBA may offer an effective tool to clarify the impact of intestinal microbiota on brain functions, in physiological and pathological conditions. In this perspective, developing an OOC-based 3D system modeling brain tissue is particularly challenging.[4]

Starting from the scalability of the thickness of COLL-based semi-IPNs to the millimeter scale and their suitability for dynamic culture in a microfluidic, optically accessible OOC device,[5] we set up a novel 3D brain-like tissue model potentially suitable for dynamic culture by coupling 1.5 mm-thick COLL-based semi-IPNs to the co-culture of cortical neurons and glial cells. Semi-IPNs have the advantage of easy tunability of their final properties,[35] a key point when aiming at co-culturing different cell types, including neural cells.

Initially, we investigated the biocompatibility of the COLL-based semi-IPNs with primary mouse microglia, neurons and astrocytes as single cultures. Compared to Matrigel, widely exploited as a scaffold material for neural cells,[39,44,45] COLL has a more defined composition and has also been successfully applied for brain cultures.[46,47]

Since different 3D culture conditions are reported[31,32] and their advantages depend on the application,[48] we considered both a layered-based model, where cells are covered by the hydrogel, and an embedded-based model, where cells are uniformly dispersed in the 3D volume. In both conditions, neurons maintained their phenotype and showed more interconnected networks than in 2D cultures. However, more complex neuronal networks and the absence of microglial activation due to the hydrogel were found in the embedded condition, indicating that it is preferable. We therefore co-cultured neurons and glial cells only in the embedded-based situation. For both embedded neurons and microglial cells, PEG-based gels performed better. In COLL-HA semi-IPNs, neuron viability was reduced, as indicated by the failure to emit extensions and build a complex network in confocal imaging and the low expression of synaptic proteins. However, astrocytes proliferated more in COLL-HA semi-IPNs. This is a key point with a view to co-culturing neurons and glial cells, since excessive astrocyte proliferation could hinder neuronal survival. With this in mind, PEG-based formulations may be the best-balanced solution also for astrocyte culture.

The importance of astrocyte-neuron ratio was reported by Fang and colleagues, who showed that the spatial relationships between neurons and astrocytes affect neuronal growth and functions.[48] To mimic the ratio between the number of glial cells and neurons in the natural brain cortex,[49] they co-cultured astrocytes and neurons on a 1:2 ratio for 14 days and showed that neurons benefited from astrocytes when these were confined by the neurons. In contrast, in the embedded condition, astrocytes over-expanded and hindered neuronal growth.[49] To avoid this, in the co-culture we used fewer glial cells than in single cultures and optimized a ratio of 1:10 between glial cells and neurons. This ratio was also considered in other studies, for instance with induced-pluripotent stem cells (iPSC).[50]

An important point when developing 3D brain cell models is to achieve sufficiently long-lasting viability to allow cell maturation and full differentiation. In our models, MTS assay confirmed cell viability up to 21 days, with a better performance for PEG-based gels. Although metabolic activity was greater for cells in COLL-PEG_{3350}, we suggest COLL-PEG_{2000} as the best option for the full 3D model because of the better structured neuron/glia networks. For this reason, it appeared as the most promising candidate for a 3D brain-like tissue model and would also be suitable to study the impact of intestinal microbiota on brain function in an OOC device. However, a further characterization of the model is mandatory, in particular by performing microglia immunostaining with suitable antibodies (e.g., CD11b or Iba1).

From the cell model point of view, primary cells are more physiological than continuous cell lines and have some advantages in terms of costs and reproducibility compared to other systems, such as those based on stem cells. The literature reports several examples of 3D brain-like tissue models exploiting stem cells, where cell differentiation is achieved with differentiation media or based on a combination of hydrogel formulation and final mechanical properties.[51–53] Recent works have focused on iPSC, which can be differentiated into neural progenitor cells, and then various CNS-related cell phenotypes. They are excellent candidates for personalized medicine[54] and disease modeling.[55–57] For instance, starting from the work by Choi et al.,[40] Park et al. employed iPSC to successfully reproduce dynamic neural-glial interactions in a microfluidic device and recapitulate key features of Alzheimer's disease, such as beta-amyloid accumulation, phosphorylated tau aggregation and neuroinflammation.[57]

However, the differentiation of iPSC-derived progenitor or precursor cells is hard to control,[58] and iPSC-derived neuronal cells are still not suitable for time-consuming optimization studies such as the one presented here, because they are expensive. Furthermore, although the differentiation protocols have been optimized to confirm the nature of post-differentiation cells in terms of functionality and morphology, the technologies still need improvements to boost reproducibility.[59] In the future, the use of commercial iPSC-derived microglial cells will extend the limited culture time of their primary counterparts, thus overcoming a current limitation of our study and improving the predictability of the 3D systems. Abud et al. described the generation of highly pure iPSC-derived human microglial-like cells similar to both fetal and adult microglia to study their functions in physiological and pathological conditions, like Alzheimer's disease.[60]

When recapitulating brain physiology at the molecular and functional levels, key points are the evaluation of synaptic proteins, suggesting the maturation of the neural network, and the recording of electrophysiological activity. For electroactive cells in 2D conditions, the recording of electrophysiological activity is widely consolidated,[32,61] while the development and optimization of electrodes and stimulation/recording devices for cells in 3D conditions is an active research field. Since the possibility of stimulating or recording relies on close proximity to the electrodes, the thickness of the culture system is important for the feasibility and reliability of the acquisition. Commercial electrodes penetrate 50 to 100 µm into the tissue, but electrophysiological measurements are reported for thicker systems. Frega et al. stacked 5-8 layers of microbeads with diameter about 40 µm and hippocampal neurons,[62] while recently Soscia et al. developed and validated an integrated 3D microelectrode array[63] for applications with 750 to 1000 µm-thick cell-loaded hydrogels. For our goals, we preliminarily investigated our 3D brain-like models using a standard electrophysiology apparatus with a patch-clamp setup, but the background noise was too high to distinguish signals from the embedded cells. Thus, further experiments and technical improvements are still needed.

Conclusions

We developed an in vitro physiological brain-like tissue model based on 1.5 mm-thick hydrogels and primary neuronal cells, also co-cultured, in both layered and embedded conditions. It provides a 3D model for setting up a brain compartment to be inserted into a complex OOC platform recapitulating brain functional relationship with peripheral body districts, as in the MGBA, in pathological and physiological conditions.

Future developments will focus on exploiting these results to develop a 3D, iPSC-based, brain-like tissue model, also for investigating Alzheimer's disease.

Acknowledgements

The authors are very grateful to Elena Restelli and Paola Fabbrizio (Istituto di Ricerche Farmacologiche Mario Negri IRCSS, Milan) for useful suggestions about cell culturing. We also thank Felice Volpe (Altergon Italia srl, Morra De Sanctis, Italy; currently at IBSA Institut Biochimique SA. Lugano, Switzerland) for suggestions about HA handling and processing and Dr. Judith Baggott for her skilled English editing.

Author contributions

IR, DA and CG conceived the study. IR carried out the experiments with support from MT for hydrogel preparation. IR and MT wrote the manuscript. GF made the equipment at the Dept. Neuroscience, Istituto di Ricerche Farmacologiche Mario Negri IRCCS, available for the experiments. DA and CG supervised the present manuscript and the related project activities. All authors discussed the results and approved the final manuscript.

Declaration of conflicting interests

The author(s) declared no potential conflicts of interest with respect to the research, authorship, and/or publication of this article.

Funding

The author(s) disclosed receipt of the following financial support for the research, authorship, and/or publication of this article: This study was funded by the European Research Council (ERC) under the European Union's Horizon 2020 research and innovation program (G.A. 724734-MINERVA) to CG. The results reflect only the authors' views and the Agency is not responsible for any use that may be made of the information contained.

ORCID iD

Marta Tunesi https://orcid.org/0000-0003-2507-6186

References

1. Sherwin E, Rea K, Dinan TG, et al. A gut (microbiome) feeling about the brain. *Curr Opin Gastroenterol* 2016; 32(2): 96–102.
2. Lerner A, Neidhöfer S and Matthias T. The gut microbiome feelings of the brain: a perspective for non-microbiologists. *Microorganisms* 2017; 5(4): 66.
3. Farzi A, Fröhlich EE and Holzer P. Gut microbiota and the neuroendocrine system. *Neurotherapeutics* 2018; 15(1): 5–22.
4. Raimondi I, Izzo L, Tunesi M, et al. Organ-On-A-Chip *in vitro* models of the brain and the blood-brain barrier and their value to study the Microbiota-Gut-Brain Axis in neurodegeneration. *Front Bioeng Biotechnol* 2020; 7: 435.
5. Tunesi M, Izzo L, Raimondi I, et al. A miniaturized hydrogel-based *in vitro* model suitable for dynamic culturing of human cells overexpressing beta-amyloid precursor protein. *J Tissue Eng* 2020; 11: 1–17.
6. Huh D, Hamilton GA and Ingber DE. From 3D cell culture to organs-on-chips. *Trends Cell Biol* 2011; 21(12): 745–754.
7. Moyer MW. Organs-on-a-Chip. *Sci Am* 2011; 304(3): 19.

8. Rothbauer M, Rosser JM, Zirath H, et al. Tomorrow today: organ-on-a-chip advances towards clinically relevant pharmaceutical and medical in vitro models. *Curr Opin Biotechnol* 2019; 55: 81–86.
9. Irons HR, Cullen DK, Shapiro NP, et al. Three-dimensional neural constructs: a novel platform for neurophysiological investigation. *J Neural Eng* 2008; 5(3): 333–341.
10. Frampton JP, Hynd MR, Shuler ML, et al. Fabrication and optimization of alginate hydrogel constructs for use in 3D neural cell culture. *Biomed Mater* 2011; 6(1): 015002.
11. Kunze A, Giugliano M, Valero A, et al. Micropatterning neural cell cultures in 3D with a multi-layered scaffold. *Biomaterials* 2011; 32(8): 2088–2098.
12. Ren M, Du C, Herrero Acero E, et al. A biofidelic 3D culture model to study the development of brain cellular systems. *Sci Rep* 2016; 6(1): 24953.
13. Paşca SP. Assembling human brain organoids. *Science* 2019; 363(6423):126–127.
14. Koo B, Choi B, Park H, et al. Past, present, and future of brain organoid technology. *Mol Cells* 2019; 42(9): 617–627.
15. Korhonen P, Malm T and White AR. 3D human brain cell models: New frontiers in disease understanding and drug discovery for neurodegenerative diseases. *Neurochem Int* 2018; 120: 191–199.
16. Camp JG, Badsha F, Florio M, et al. Human cerebral organoids recapitulate gene expression programs of fetal neocortex development. *Proc Natl Acad Sci U S A* 2015; 112(51): 15672–15677.
17. Yin X, Mead BE, Safaee H, et al. Engineering stem cell organoids. *Cell Stem Cell* 2016; 18(1): 25–38.
18. Tomaskovic-Crook E and Crook JM. Clinically amendable, defined, and rapid induction of human brain organoids from induced pluripotent stem cells. *Methods Mol Biol* 2019; 1576: 13–22.
19. George J, Hsu CC, Nguyen LTB, et al. Neural tissue engineering with structured hydrogels in CNS models and therapies. *Biotechnol Adv*. Epub ahead of print March 2019. DOI: 10.1016/j.biotechadv.2019.03.009.
20. Engler AJ, Sen S, Sweeney HL, et al. Matrix elasticity directs stem cell lineage specification. *Cell* 2006; 126(4): 677–689.
21. Saha K, Keung AJ, Irwin EF, et al. Substrate modulus directs neural stem cell behavior. *Biophys J* 2008; 95(9): 4426–4438.
22. Balgude AP, Yu X, Szymanski A, et al. Agarose gel stiffness determines rate of DRG neurite extension in 3D cultures. *Biomaterials* 2001; 22(10): 1077–1084.
23. Willits RK and Skornia SL. Effect of collagen gel stiffness on neurite extension. *J Biomater Sci Polym Ed* 2004; 15(12): 1521–1531.
24. Gunn JW, Turner SD and Mann BK. Adhesive and mechanical properties of hydrogels influence neurite extension. *J Biomed Mater Res A* 2005; 72(1): 91–97.
25. Watanabe K, Nakamura M, Okano H, et al. Establishment of three-dimensional culture of neural stem/progenitor cells in collagen Type-1 Gel. *Restor Neurol Neurosci* 2007; 25(2): 109-117.
26. Pires LR, Rocha DN, Ambrosio L, et al. The role of the surface on microglia function: implications for central nervous system tissue engineering. *J R Soc Interface* 2015; 12(103): 20141224.
27. Tremblay MÈ, Lowery RL and Majewska AK. Microglial interactions with synapses are modulated by visual experience. *PLoS Biol* 2010; 8(11): e1000527.
28. Schafer DP, Lehrman EK, Kautzman AG, et al. Microglia sculpt postnatal neural circuits in an activity and complement-dependent manner. *Neuron* 2012; 74(4): 691–705.
29. David S and Kroner A. Repertoire of microglial and macrophage responses after spinal cord injury. *Nat Rev Neurosci* 2011; 12(7): 388–399.
30. Leung BK, Biran R, Underwood CJ, et al. Characterization of microglial attachment and cytokine release on biomaterials of differing surface chemistry. *Biomaterials* 2008; 29(23): 3289–3297.
31. Ylä-Outinen L, Joki T, Varjola M, et al. Three-dimensional growth matrix for human embryonic stem cell-derived neuronal cells. *J Tissue Eng Regen Med* 2014; 8(3): 186–194.
32. Xu T, Molnar P, Gregory C, et al. Electrophysiological characterization of embryonic hippocampal neurons cultured in a 3D collagen hydrogel. *Biomaterials* 2009; 30(26): 4377–4383.
33. Balasubramanian S, Packard JA, Leach JB, et al. Three-dimensional environment sustains morphological heterogeneity and promotes phenotypic progression during astrocyte development. *Tissue Eng Part A* 2016; 22(11–12): 885–898.
34. Tunesi M, Batelli S, Rodilossi S, et al. Development and analysis of semi-interpenetrating polymer networks for brain injection in neurodegenerative disorders. *Int J Artif Organs* 2013; 36(11): 762–774.
35. Tunesi M, Raimondi I, Russo T, et al. Hydrogel-based delivery of Tat-fused protein Hsp70 protects dopaminergic cells in vitro and in a mouse model of Parkinson's disease. *NPG Asia Mater* 2019; 11(1): 1–15.
36. Saura J, Tusell JM and Serratosa J. High-yield isolation of murine microglia by mild trypsinization. *Glia* 2003; 44(3): 183–189.
37. Apolloni S, Parisi C, Pesaresi MG, et al. The NADPH oxidase pathway is dysregulated by the P2X7 receptor in the SOD1-G93A microglia model of amyotrophic lateral sclerosis. *J Immunol* 2013; 190(10): 5187–5195.
38. Restelli E, Fioriti L, Mantovani S, et al. Cell type-specific neuroprotective activity of untranslocated prion protein. *PLoS One* 2010; 5(10): e13725.
39. Bohlen CJ, Bennett FC, Tucker AF, et al. Diverse requirements for microglial survival, specification, and function revealed by defined-medium cultures. *Neuron* 2017; 94(4): 759–773.e8.
40. Choi SH, Kim YH, Hebisch M, et al. A three-dimensional human neural cell culture model of Alzheimer's disease. *Nature* 2014; 515(7526): 274–278.
41. Pani G, Samari N, Quintens R, et al. Morphological and physiological changes in mature in vitro neuronal networks towards exposure to short-, middle- or long-term simulated microgravity. *PLoS One* 2013; 8(9): e73857.
42. Edmondson R, Adcock AF and Liju Y. Influence of matrices on 3D-cultured prostate cancer cells' drug response and expression of drug-action associated proteins. *PLoS One* 2016; 11(6): e0158116.
43. Mimee M, Citorik RJ and Lu TK. Microbiome therapeutics – advances and challenges. *Adv Drug Deliv Rev* 2016; 105: 44–54.

44. Yan W, Liu W, Qi J, et al. A three-dimensional culture system with matrigel promotes purified spiral ganglion neuron survival and function in vitro. *Mol Neurobiol* 2018; 55(3): 2070–2084.
45. Wang J, Chu R, Ni N, et al. The effect of Matrigel as scaffold material for neural stem cell transplantation for treating spinal cord injury. *Sci Rep* 2020; 10(1): 2576.
46. Kothapalli CR and Kamm RD. 3D matrix microenvironment for targeted differentiation of embryonic stem cells into neural and glial lineages. *Biomaterials* 2013; 34(25): 5995–6007.
47. Bourke JL, Quigley AF, Duchi S, et al. Three-dimensional neural cultures produce networks that mimic native brain activity. *J Tissue Eng Regen Med* 2018; 12(2): 490–493.
48. Fang A, Li D, Hao Z, et al. Effects of astrocyte on neuronal outgrowth in a layered 3D structure. *Biomed Eng Online* 2019; 18(1): 74.
49. Herculano-Houzel S. The glia/neuron ratio: how it varies uniformly across brain structures and species and what that means for brain physiology and evolution. *Glia* 2014; 62(9): 1377–1391.
50. Tukker AM, Wijnolts FMJ, de Groot A, et al. Human iPSC-derived neuronal models for in vitro neurotoxicity assessment. *Neurotoxicology* 2018; 67: 215–225.
51. Seidlits SK, Khaing ZZ, Petersen RR, et al. The effects of hyaluronic acid hydrogels with tunable mechanical properties on neural progenitor cell differentiation. *Biomaterials* 2010; 31(14): 3930–3340.
52. Aurand ER, Wagner JL, Shandas R, et al. Hydrogel formulation determines cell fate of fetal and adult neural progenitor cells. *Stem Cell Res* 2014; 12(1): 11–23.
53. Knowlton S, Cho Y, Li XJ, et al. Utilizing stem cells for three-dimensional neural tissue engineering. *Biomater Sci* 2016; 4(5): 768–784.
54. Walker MJ, Bourke J and Hutchison K. Evidence for personalised medicine: mechanisms, correlation, and new kinds of black box. *Theor Med Bioeth* 2019; 40(2): 103–121.
55. Peng SP and Copray S. Comparison of human primary with human iPS cell-derived dopaminergic neuron grafts in the rat model for Parkinson's disease. *Stem Cell Rev Rep* 2016; 12(1): 105–120.
56. Zhang ZN, Freitas BC, Qian H, et al. Layered hydrogels accelerate iPSC-derived neuronal maturation and reveal migration defects caused by MeCP2 dysfunction. *Proc Natl Acad Sci U S A* 2016; 113(12): 3185–3190.
57. Park J, Wetzel I, Marriott I, et al. A 3D human triculture system modeling neurodegeneration and neuroinflammation in Alzheimer's disease. *Nat Neurosci* 2018; 21(7): 941–951.
58. Wu S, Xu R, Duan B, et al. Three-dimensional hyaluronic acid hydrogel-based models for in vitro human iPSC-derived NPC culture and differentiation. *J Mater Chem B* 2017; 5(21): 3870–3878.
59. Farkhondeh A, Li R, Gorshkov K, et al. Induced pluripotent stem cells for neural drug discovery. *Drug Discov Today* 2019; 24(4): 992–999.
60. Abud EM, Ramirez RN, Martinez ES, et al. iPSC-derived human microglia-like cells to study neurological diseases. *Neuron* 2017; 94(2): 278–293.
61. Gouwens NW, Sorensen SA, Berg J, et al. Classification of electrophysiological and morphological neuron types in the mouse visual cortex. *Nat Neurosci* 2019; 22(7): 1182–1195.
62. Frega M, Tedesco M, Massobrio P, et al. Network dynamics of 3D engineered neuronal cultures: a new experimental model for in-vitro electrophysiology. *Sci Rep* 2014; 4: 5489.
63. Soscia DA, Lam D, Tooker AC, et al. A flexible 3-dimensional microelectrode array for in vitro brain models. *Lab Chip* 2020; 20(5): 901–911.